Uridine Diphosphate (UDP) Promotes Rheumatoid Arthritis Through P2Y6 Activation

Hongxing Wang
Qingdao University
Hui Wu
Qingdao University
Kehua Fang
Qingdao University
Xiaotian Chang (changxt@126.com)
Qindao University https://orcid.org/0000-0002-7639-7740

Research article

Keywords: Uridine diphosphate (UDP), Immunohistochemistry

Posted Date: August 12th, 2020

DOI: https://doi.org/10.21203/rs.3.rs-56879/v1

Version of Record: A version of this preprint was published at Frontiers in Pharmacology on April 19th, 2021. See the published version at https://doi.org/10.3389/fphar.2021.658511.

Abstract

Background: Uridine diphosphate (UDP) is an extracellular nucleotide signaling molecule implicated in diverse biological processes via specific activation of the metabotropic pyrimidine and purine nucleotide receptor pyrimidinergic receptor P2Y, G Protein-Coupled, 6 (P2Y6).

Methods: This study used a quasi-targeted liquid chromatography-mass spectrometry (LC-MS) approach to investigate the unique expression of metabolites in rheumatoid arthritis (RA) synovial fluid (SF) (n=10) with samples from osteoarthritis (OA) as controls (n=10). RA fibroblast-like synoviocytes (FLSs) were collected from synovial tissues and cultured with UDP or MRS2578, P2Y6 antagonist, and FLSs from OA was used as controls. Rats with collagen-induced arthritis (CIA) were established and injected with UDP or MRS2578 or both. P2Y6 expression was examined using real-time PCR, Western blotting and Immunohistochemistry. Cell proliferation, apoptosis and migration of FLSs were measured using CCK-8 assay, real-time cell analysis, flow cytometry, the wound healing assay and transwell assay. The concentration of UDP in culture medium, synovial fluid and peripheral blood RA and CIA rats was measured using a Transcreener UDP Assay, IL-6 was measured using ELISA and flow assay, and other pro-inflammatory cytokines was measured using Th1/Th2 Subgroup Detection Kit.

Results: LC-MS analysis showed that the UDP level is not only higher in RA SF than in OA SF but also positively correlated with anticyclic citrullinated peptide (anti-CCP) and rheumatoid factor (RF) levels in RA. The increased UDP concentration was verified in the plasma and SF samples of RA patients (n=36) and healthy volunteers (n=36), and the levels were significantly correlated with RF and anti-CCP level in the samples. The study also found that UDP stimulated the cell proliferation, migration and interleukin-6 (IL-6) secretion of RA FLSs and inhibited their apoptosis in the culture. The P2Y6 antagonist MRS2578 inhibited this effect of UDP in the culture. UDP injection accelerated the development of collagen-induced arthritis (CIA) in a rat model and stimulated IL-6 production, but simultaneous injection of MRS2578 suppressed these effects and alleviated CIA. P2Y6 expression was increased in RA and CIA synovial tissues and was unaltered by UDP treatment. UDP treatment and P2Y6 activity didn’t change levels of other proinflammatory cytokines in cultured FLSs and CIA rats.

Conclusion: These results suggest that UDP is highly expressed in RA and stimulates RA pathogenesis by promoting P2Y6 activities to increase IL-6 production.

Background

Rheumatoid arthritis (RA) is a chronic and systemic autoimmune inflammatory disease [1]. Synovial fluid (SF) accumulates extensively in the synovial junctions in individuals with RA. SF directly contacts the joint; therefore, it reflects the pathological state of the synovium and disease activity. The present study used metabolomics as a high-throughput approach to analyze changes in small molecular metabolites in SF samples from RA patients. We collected SF samples by aspiration from 10 patients with RA and 10 patients with osteoarthritis (OA). Quasi-targeted liquid chromatography-mass spectrometry (LC-MS), an

advanced metabolomics technique that was developed in recent years, was applied to screen unique expression of metabolites in RA SF. After the metabolomic analysis, uridine diphosphate (UDP) was found to be present at a high level in RA SF.

UDP molecules comprise a pyrophosphate, a ribose and a uracil group with the pyrophosphate esterified to the C5 carbon of the sugar moiety. UDP is an important extracellular nucleotide signaling molecule [2] implicated in diverse biological processes via specific activation of the metabotropic pyrimidine and purine nucleotide receptor (P2Y receptor) subtype P2Y6 [3–5]. Previous studies have shown that extracellular UDP is released from damaged or stressed cells to promote innate immune responses [7, 8]. However, the function and mechanism of extracellular UDP in RA remain unknown. In this study, we also investigated the role of UDP/P2Y6 signaling in RA using cultured RA fibroblast-like synoviocytes (FLSs) and a rat model of collagen-induced arthritis (CIA). Abnormal FLS proliferation is the main characteristic of RA pathogenesis. FLSs have a major effect on the pathogenesis of RA mediated by their aggressive proliferation and production of proinflammatory cytokines such as interleukin-6 (IL-6) [9–13]. Diisothiocyanate (MRS2578), with an IC50 value of 37 nM, is a powerful antagonist of the nucleotide receptor P2Y6 [6]. We thus treated RA FLSs and CIA rats with UDP and MRS2578 to observe the potential changes in synovial cell proliferation and migration, CIA-related joint inflammation and tissue destruction, and cytokine production. In summary, this study aimed to investigate the role and regulatory mechanism of UDP in RA.

Methods

Collection of human SF and synovial tissues

RA was diagnosed according to the American College of Rheumatology/European League Against Rheumatism (ACR/EULAR) classification criteria [14, 15]. Human blood (n = 36) and SF (n = 36) were collected from patients with RA. RA synovial membrane tissues were collected from the patients (n = 9) during knee joint arthroscopic synovectomy. The use of samples for research was approved by The Ethics Committee of The Affiliated Hospital of Qingdao University (approval number: 20190302). All patients who joined this study provided informed consent. The clinical information of the patients with RA is provided in **Supplementary Table 1.**

Metabolomic profiling of SF

Sex-matched SF samples from patients with RA (10 patients; Patient No. 1 to No. 10) and OA (10 patients; Patient No. 1 to No. 10) were injected into an ACQUITY UPLC I-Class system (Waters Corporation, Milford, USA) through a BEH amide column (100 mm × 2.1 mm i.d., 1.7 m; Waters, Milford, USA) and analyzed in a VION IMS QTof mass spectrometer (Waters Corporation, Milford, USA). The LC flow rate was 0.4 mL/min with solvents A (a mixture of acetonitrile and 10 mmol ammonium acetate (pH = 9) (90/10%, volume/volume)) and B (10 mmol ammonium acetate (pH = 9)). The sample volume was 3 µL, the column temperature was held at 45 °C, and the elution gradient of solvent B was as follows: 0 min, 5%; 1.5 min, 25%; 10 min, 90%; 13 min, 90%; 13.5 min, 5% and 14.5 min, 5%. Data acquisition was

performed in full scan mode (over an m/z range of 50 to 1000), and the scan time was 0.1 seconds. The capillary voltage was 1.0 kV, and the sampling cone voltage was 40 V. The source temperature was 120 °C. The desolvation temperature was 550 °C, and the flow rate of the desolvation gas was 900 L/hour. To assess the stability of the system, quality control (QC) samples were injected at regular intervals throughout the analysis operation. Volcano plots were generated by analyzing the fold change (FC) and p values from the t-test results and the variable importance in projection (VIP) scores from orthogonal partial least squares discriminant analysis (OPLS-DA). Metabolites meeting the criteria of VIP > 1, FC > 2 or < 0.5 and $p < 0.05$ were defined as differentially expressed metabolites (DEMs).

Weighted gene coexpression network analysis (WGCNA)

WGCNA was performed with R software (v3.6.1). The correlation coefficients of all metabolites were calculated according to their expression values, and a soft thresholding power ($\beta = 8$) was selected. The coexpression similarity was mapped into a weighted undirected network and topological overlap matrix (TOM). The dynamic tree cut algorithm was used to cluster metabolites into modules. The following parameters were used: MaxBlockSize, 6000; TOMType, unsigned; and minModuleSize, 30.

Establishment of CIA in rats

Six-week-old male Sprague-Dawley (SD) rats were purchased from JNPY Laboratory Animal Co., Ltd. (Jinan, China). The animal study protocols complied with the Guide for the Care and Use of Laboratory Animals [16] and were approved by the Experimental Animal Care and Ethics Committee of The Affiliated Hospital of Qingdao University (approval number: 20190302). These rats were randomly divided into a normal control (NC) group and CIA control group. Bovine type II collagen (Chondrex, USA) was mixed with complete Freund's adjuvant (Sigma-Aldrich, Germany) and fully emulsified. The initial immunization was performed by intracutaneous injection at the tail root. Three weeks later, a booster immunization was administered using a mixture of bovine type II collagen and incomplete Freund's adjuvant (Sigma-Aldrich, Germany). The next week, rats with successful establishment of CIA were randomly divided into a PBS treatment group (n = 9), a UDP treatment group (n = 9), an MRS2578 treatment group (n = 9), and a UDP (Sigma-Aldrich, Germany) and MRS2578 (MedChemExpress, USA) treatment group (n = 9). UDP and MRS2578 were dissolved in PBS (containing 1% DMSO) as the vehicle. Rats in the UDP treatment group were injected intraperitoneally with UDP (10 mg/kg). Rats in the MRS2578 treatment group were injected intraperitoneally with MRS2578 solution (3 mg/kg). Rats in the UDP and MRS2578 treatment group were injected with the same volume of a solution containing UDP (10 mg/kg) and MRS2578 (3 mg/kg). Rats in the PBS treatment group were injected with the same volume of PBS vehicle (containing 1% DMSO). Injections were performed twice weekly for a total of 6 consecutive administrations. The inflammation curve showing the degree of joint swelling with time was constructed.

Rats were anesthetized by intraperitoneal injection of 3% sodium pentobarbital, and blood samples were collected from the inferior vena cava. In addition, the articular cavity of the rats was washed 3 times with PBS (1 mL) to collect SF. These rats were euthanized with lethal doses of ketamine and xylazine, and the joint tissues within 0.5 cm of the knee joints were collected.

Evaluation of joint inflammation

Rats were sacrificed 20 days after the first UDP injection. The inflammation curve was constructed according to the size of the hind paws, which was measured every other day using Vernier calipers. Bone erosion and cartilage destruction in the ankle joint and knee joint were assessed by X-ray imaging (75 kV, 195.3 mA) before sacrifice. The joint tissue within 0.5 cm of the knee joint of rats was collected, fixed with 4% paraformaldehyde and embedded in paraffin. Hematoxylin-eosin staining was used to examine the pathological changes in joint tissues. According to clinical and histological evidence, the disease score is calculated as follows: 0 = normal joint; 1 = local swelling and/or erythema without histological damage; 2 = swelling and/or rigidity of the whole paw without histological damage; 3 = limb deformity with reversible histological damage; 4 = limb deformity accompanied by permanent histological damage such as bone or cartilage erosion.

Isolation and culture of human FLSs

Synovial tissue samples from patients with RA (Patient No. 25 to No. 36, n = 12) or OA (Patient No. 25 to No. 36, n = 12) were minced into small pieces and digested for 4 h at 37 °C and 5% CO_2 in 3 mL of DMEM containing 4% type II collagenase (Solarbio, China) until the tissue pieces were dispersed into a cell suspension. The cell suspension was filtered through a 70 μm cell strainer and resuspended in DMEM containing 10% FBS. FLSs were incubated at 37 °C in a humidified incubator containing 5% CO_2. Cells passed for 3–8 generations were used in subsequent experiments.

Measurement of UDP content

Peripheral blood samples from healthy donors and RA patients (Patient No. 1 to No. 36, n = 36) were collected into pyrogen-free and endotoxin-free test tubes with anticoagulants. SF samples from OA and RA patients (Patient No. 1 to No. 36, n = 36) were added to an equal volume of PBS. Rat SF and plasma were collected as described above. These samples were centrifuged at 1000 × g for 20 min at 4 °C, and the supernatant was carefully collected. The UDP content in the samples was measured using a Transcreener UDP Assay (BellBrook Labs, USA) via a fluorescence polarization readout according to the manufacturer's protocol. A 15 μL mixture of reagents, including 8 nm UDP^2 antibody-Tb, 1 × Stop & Detect Buffer C and UDP HiLyte647 Tracer, was mixed with 5 μL of each sample in a 96-well plate. The plate was incubated for 1.5 h at room temperature and analyzed in a FlexStation® 3 Multimode Plate Reader (Molecular Devices, USA). The concentration of UDP was calculated by the standard curve prepared with standard UDP solution before analysis.

Measurement of cytokine concentrations in blood and culture medium

RA FLSs (Patient No. 1 to No. 5, n = 5) were seeded in 96-well plates at a density of 3×10^4 cells per well and incubated overnight. UDP was dissolved in PBS (containing 0.1% DMSO). Cells were incubated with UDP at a final concentration of 100 μM for 24 h. The supernatants were collected after centrifugation at

1000 × g for 20 min. The IL-2, IL-4, IL-6, IL-10, TNF-α and IFN-γ concentrations in the supernatants were quantified using a Human Th1/Th2 Subgroup Detection Kit (CellGene, China). In brief, antibodies specific for IL-2, IL-4, IL-6, IL-10, TNF-α and IFN−γ were conjugated to fluorescence-encoded beads, and beads with the biotinylated detection antibodies were mixed with the samples. Streptavidin-PE was added, and the mixture was incubated with shaking for 2 h at room temperature. The beads were washed and were then analyzed in a NovoCyte D2040R flow cytometer (ACEA Biosciences, USA). The data were analyzed using FlowJo software (Tree Star, USA).

Measurement of IL-6 levels using enzyme-linked immunosorbent assay (ELISA)

RA FLSs and OA FLSs (Patient No. 1 to No. 5, n = 5) were treated with different concentrations (0 μM, 10 μM, 50 μM and 100 μM) of UDP (Sigma-Aldrich, Germany), and the supernatants were collected at 24 h. The concentration of IL-6 was measured with an ELISA kit (eBioscience, USA) according to the protocol. In brief, a 100 μL volume of the standard, control or sample was added to each well and incubated for 2 h at room temperature. After three washes, 200 μL of human IL-6 conjugate antibody was added to each well, incubated for 2 h at room temperature and washed three times. A 200 μL aliquot of substrate solution was then added to each well and incubated for 20 min at room temperature. Then, 50 μL of Stop Solution was added to each well, and the optical density of each well was measured at 450 nm in a microplate reader (BioTek, USA).

Measurement of IL-6 levels using flow assay

RA FLSs (Patient No. 1 to No. 5, n = 5) were seeded in 96-well plates at a density of 3×10^4 cells per well and incubated overnight. UDP and MRS2578 were dissolved in PBS vehicle containing 0.1% DMSO. Cells were incubated with or without MRS2578 (Med Chem Express, USA) at a final concentration of 10 μM for 1 h. UDP (Sigma-Aldrich, Germany) was then added at a final concentration of 100 μM, and incubation was continued for 24 h. The supernatants were collected after centrifugation at 1000 × g for 20 min. The IL-6 concentrations in the supernatants were quantified using a human IL-6 flow assay kit (Cell Gene, China). In brief, anti-IL-6 antibodies were conjugated to fluorescence-encoded beads, and the beads and biotinylated anti-IL-6 detection antibodies were mixed with the samples. Streptavidin-PE was added, and the mixture was incubated with shaking for 2 h at room temperature. The beads were washed and were then analyzed in a NovoCyte D2040R flow cytometer (ACEA Biosciences, USA). The data were analyzed using FlowJo software (Tree Star, USA).

Rat plasma was collected from the inferior vena cava, and the IL-6 level was measured using a similar protocol with the rat IL-6 capture bead B6 product commercially obtained from BioLegend. The data were analyzed using LEGENDplex v8.0 software (BioLegend).

Evaluation of FLS proliferation by a CCK-8 assay

RA FLSs and OA FLSs (Patient. 1 to No. 5, n = 5) were treated with different concentrations (0 μM, 10 μM, 50 μM or 100 μM) of UDP for 0, 6, 12 and 24 h. A 10 μL volume of CCK-8 solution (Dojindo, Japan) was

added to each well and incubated for an additional 4 h. The absorbance was measured at 450 nm in a spectrophotometer (BioTek, USA).

Evaluation of FLS proliferation using real-time cell analysis (RTCA)

A dual-plate RTCA instrument (ACEA Biosciences, USA) (Patient No. 6 to No. 10 n = 5) was placed in a humidified incubator maintained at 37 °C and 5% CO_2. RA FLSs were seeded in cell culture E-plates (1×10^4 cells per well) (ACEA Biosciences, USA) and treated with 100 μM UDP with or without MRS2578 at a final concentration of 10 μM for 3 days. The 96-well E-plate was monitored every 30 min for 48 h, and cell proliferation was monitored in real time by measuring the electrical impedance using the xCELLigence RTCA TP System (ACEA Biosciences, USA). The cell growth curves were automatically recorded based on continuous quantitative monitoring of cell proliferation. The data were analyzed with Real-Time Cell Analyzer software (version 1.2).

Detection of FLS apoptosis via flow cytometry

RA FLSs and OA FLSs (Patient No. 6 to No. 10, n = 5) were treated with or without MRS2578 (MedChemExpress, USA) at a final concentration of 10 μM for 1 h. Then, UDP at a final concentration of 100 μM was added, and incubation was continued for 24 h. Cells (6×10^4) were then collected and resuspended in binding buffer. An Annexin V-FITC-conjugated antibody and a PI-conjugated antibody (BioLegend) were then added to the suspended cells. Apoptosis was detected by flow cytometry.

Cell migration assay

RA FLSs and OA FLSs (Patient No. 6 to No. 10, n = 5) were seeded in 6-well plates. When the cells were 80–90% confluent, the wound healing assay was conducted by scratching the cell layer in each well with a sterile P200 pipette tip. The cells were preincubated with or without MRS2578 (MedChemExpress, USA) at a final concentration of 10 μM for 1 h. UDP at a final concentration of 100 μM was then added, and incubation was continued for 24 h. The cells were photographed at 0 h and 24 h (Olympus IX51, Japan), and the wound area was calculated with ImageJ software (NIH, Bethesda, MD, USA).

Transwell assay

RA FLSs and OA FLSs (Patient No. 6 to No. 10, n = 5) (1×10^4 cells/mL) in serum-free medium were seeded in the upper compartments of Matrigel Invasion Chambers (Corning, USA). Medium containing 10% FBS was added to the lower compartments of the chambers. The cells were incubated with or without MRS2578 (MedChemExpress, USA) at a final concentration of 10 μM for 1 h. UDP (Sigma-Aldrich, Germany) at a final concentration of 100 μM was then added, and incubation was continued for 24 h. The cells on the top surface of the membrane were removed with cotton swabs, and cells that penetrated to the bottom surface of the membrane were stained with crystal violet. Images were acquired by fluorescence microscopy (Olympus IX51, Japan), and the cells were quantified with ImageJ software (NIH, Bethesda, MD, USA).

Sources of microarray data

The expression level of P2Y6 in RA and OA synovial tissue was analyzed in four published gene expression profile datasets (dataset type: expression profiling by array) in the Gene Expression Omnibus (GEO, https://www.ncbi.nlm.nih.gov/geoprofiles) database. The expression data of 10 patients with RA and 6 OA controls from dataset GDS5402/208373_s_at, 5 patients with RA and 5 OA controls from dataset GDS2126/38222_at, 10 patients with RA and 10 OA controls from dataset GDS5401/208373_s_at, and 13 patients with RA and 10 OA controls from dataset GDS5403/208373_s_at were analyzed in SPSS software v. 21.0 (IBM, USA) using an unpaired Student's t-test.

RNA isolation and quantitative real-time PCR (Q-PCR)

Human (Patient No. 11 to No. 19, n = 9) and rat synovial tissues were collected as described above. Total RNA was isolated using TRIzol reagent (Invitrogen) and reverse transcribed to cDNA (Vazyme, China). Q-PCR was performed in a StepOnePlus™ Real-Time PCR System (Thermo Fisher Scientific, USA) using iQ SYBR Green Supermix (Bio-Rad) according to the manufacturer's guidelines. The PCR primers were designed as follows: human P2Y6 sense: 5′-GTGTCTACCGCGAGAACTTCA-3′, human P2Y6 antisense: 5′-CCAGAGCAAGGTTTAGGGTGTA-3′; human β-actin sense: 5′-CATGTACGTTGCTATCCAGGC-3′, human β-actin antisense: 5′-CTCCTTAATGTCACGCACGAT-3′; rat P2Y6 sense: 5′-GTGGTATGTGGAGTCGTTTGA-3′, rat P2Y6 antisense: 5′-CTGTAGGAGATCGTGTGGTT-3′; rat GAPDH sense: 5′-TCCCTCAAGATTGTCAGCAA-3′, rat GAPDH antisense: 5′-AGATCCACAACGGATACATT-3′. The PCR primers were designed based on a study by Kim [17].

Evaluation of P2Y6 expression using Western blotting (WB)

Human synovial tissues (Patient No. 11 to No. 15, n = 5) were collected as described above. Samples were homogenized on ice in radioimmunoprecipitation assay (RIPA) lysis buffer (Beyotime), separated by 12% sodium dodecyl sulfate-polyacrylamide gel electrophoresis (SDS-PAGE) and transferred to polyvinylidene fluoride (PVDF) membranes (Millipore, USA). Membranes were incubated with a rabbit anti-P2Y6 antibody (Abcam, ab198805) and horseradish peroxidase (HRP)-conjugated goat anti-rabbit IgG (ab205718). β-Actin (Abcam, ab115777) was used as the internal reference for normalization of the P2Y6 expression level. Immunoreactive bands were visualized using Western Chemiluminescent Horseradish Peroxidase Substrate (ECL, Millipore), and band densities were quantified using ImageJ software (NIH, Bethesda, MD, USA).

Evaluation of P2Y6 expression using immunofluorescence

Paraffin sections of human synovial tissues (Patient No. 20 to No. 24, n = 5) were permeabilized with 0.05% Triton X-100 for 10 min, blocked with 5% goat serum for 1 h, and incubated with a rabbit anti-P2Y6 antibody (1:200, Abcam, ab198805) at 4 °C overnight. The tissue sections were incubated with goat anti-rabbit IgG H&L (Alexa Fluor® 555) (1:200, Abcam, ab150078) for 1 hour in the dark. Nuclei were stained with 4′,6-diamidino-2-phenylindole (DAPI) (Abcam, ab228549). Images were acquired under a

fluorescence microscope and quantification was conducted in Image-Pro Plus 6.0 (Media Cybernetics, Inc., Rockville, MD, USA).

Examination of P2Y6 expression using immunohistochemical staining

Paraffin sections of human synovial tissues (Patient No. 20 to No. 24, n = 5) were incubated first with a rabbit anti-P2Y6 antibody (1:200, Abcam, ab198805) at 4 °C overnight and then with HRP-conjugated goat anti-rabbit IgG (ab205718). Sections were then treated with diaminobenzidine (DAB) and counterstained with hematoxylin. The results were analyzed and expression was quantified in ImageJ software (NIH, Bethesda, MD, USA).

Statistical analysis

Statistical analyses were performed using GraphPad Prism 7.0 (GraphPad, USA) and SPSS software v.21.0 (IBM, USA). The significance of differences between groups was evaluated using Student's unpaired t-test. Differences with p values of < 0.05 were considered significant.

Results

Metabolomic analysis of RA SF

Samples of RA (n = 10) and OA (n = 10) SF were analyzed using an LC-MS approach. A total of 481 variables were identified after searching the Human Metabolome Database (HMDB). Orthogonal Partial Least Squares-Discriminant Analysis (OPLS-DA), the most frequently used multivariate statistical method, was applied for metabolomic analysis. The R^2Y of the OPLS-DA model was 1, and the Q^2 was 0.96, indicating that the model was stable and reliable. The OA and RA OPLS-DA score plots were separated, indicating that the model could discriminate metabolites between the OA and RA groups (Fig. 1A). Volcano plots were constructed by analyzing the fold change (FC) and p values from the t-test results, and the variable importance in projection (VIP) scores from OPLS-DA. Metabolites meeting the criteria of VIP > 1, FC > 2 or < 0.5 and $p < 0.05$ were defined as differentially expressed metabolites DEMs. The contents of the following metabolites were significantly elevated in RA SF samples compared with OA samples: 2-aminobenzoic acid, 2-hydroxy-3-methylbutyric acid, 9,12,13-TriHOME, creatinine, cyclic GMP (guanosinc monophosphate), epinephrine sulfate, guanidinosuccinic acid, guanosine, isobutyryl-L-carnitine, methionine sulfoxide, N-acetyl-L-tyrosine, norepinephrine sulfate, phenol, phenylpropanolamine, S-adenosylhomocysteine, tauroursodeoxycholic acid and UDP. In addition, the content of pyrophosphate was significantly decreased in RA samples (Fig. 1B). Using the metabolite set, we identified 8 variable network modules (green (n = 51), black (n = 31), brown (n = 56), blue (n = 66), turquoise (n = 144), red, yellow (n = 54), and gray (n = 27) via WGCNA. Each leaf in the tree represents one metabolite (Fig. 1C). Correlations between these metabolite network modules and clinical prognostic data (sex, age, rheumatoid factor (RF) level, anticyclic citrullinated peptide (anti-CCP) level, and Kellgren-Lawrence (K&L) scale score were analyzed. The turquoise module was found to be markedly positively correlated with RF

(r = 0.71, p = 0.0004) and anti-CCP (r = 0.67, p = 0.001); the red module was found to be markedly positively correlated with RF (r = 0.88, p < 0.0001) and anti-CCP (r = 0.84, p < 0.0001) levels (Fig. 1D). Cytoscape 3.6.1 was used to visualize the metabolite network in the red module. A total of 49 variables were identified in the red module: UDP, urocanic acid, thiosulfate, sulfide, ribitol, pyridoxal, pipecolic acid, phytanic acid, p-hydroxyphenylacetic acid, PC(18:3(6Z,9Z,12Z)/24:1(15Z)), paraxanthine, orotidine, ornithine, nicotinic acid, nandrolone, monoisobutyl phthalic acid, methylamine, lysoPC(14:1(9Z)), L-serine, L-proline, L-octanoylcarnitine, L-arginine, isovalerylglycine, imidazoleacetic acid, guanidine, erythritol, erucic acid, D-ribose, dimethylsulfide, dimethyl-L-arginine, dimethylglycine, D-glucuronic acid, cholesterol sulfate, chenodeoxycholic acid glycine conjugate, CE(18:2(9Z,12Z)), behenic acid, ascorbic acid, 9-OxoODE, 9,12,13-TriHOME, 7-dehydrocholesterol, 5-methoxydimethyltryptamine, 4-hydroxyphenylpyruvic acid, 4-aminophenol, 4,7,10,13,16-docosapentaenoic acid, 1-phenylethylamine, 1-methylhistidine, 14,15-DiHETE, and 1,3-diaminopropane. The results are shown in a Venn diagram (Fig. 1E). Two metabolites (UDP and 9,12,13-TriHOME) were found in both the red module identified by WGCNA and among the DEMs identified by volcano plot analysis (Fig. 1F), indicating that they might play an important role in promoting the pathological progression of RA. By analyzing the VIP scores, odds ratios (ORs) in logistic regression and FC values, we focused on the pathogenic role of UDP in the subsequent study (Fig. 1G). The above data are also provided in **Supplementary Table 2.**

UDP level in RA peripheral blood and SF

The UDP concentration was measured in the plasma of RA patients (n = 36) and healthy volunteers (n = 36) using the Transcreener UDP Assay. Compared with those in the blood of healthy volunteers (27.1 ± 2.1 ng/mL), the UDP levels in the blood of patients with RA were significantly increased (46.8 ± 7.8 ng/mL, p = 0.017) (Fig. 2A). Pearson correlation analysis was performed, and no correlation was detected (R = -0.18) between the blood UDP level and serum RF level (Fig. 2B) or between the UDP level and serum anti-CCP level (R =-0.04) (Fig. 2C). Receiver operating characteristic (ROC) analysis was used to examine possible associations between blood UDP levels and RF and anti-CCP levels in RA patients. In the ROC analysis, an area under the ROC curve (AUC) of > 0.9 was considered excellent; 0.8–0.9, very good; 0.7–0.8, good; 0.6–0.7, average; and < 0.6, poor. The AUC value of UDP was 0.97, which was thus considered to indicate an excellent diagnostic test for RA (Fig. 2D). In addition, the UDP concentration was measured in RA SF (n = 36) and OA SF (n = 36). Compared with that in OA SF (0.5 ± 0.5 ng/mL), the UDP level in RA SF was significantly increased (23.1 ± 32.9 ng/mL, p < 0.0001) (Fig. 2E). Pearson correlation analysis detected a moderate positive correlation (R = 0.75) between the SF UDP level and serum RF level (Fig. 2F) and between the SF UDP level and serum anti-CCP level (R = 0.76) (Fig. 2G).

The effect of UDP on RA FLSs

Cultured RA FLSs (n = 5) and OA FLSs (n = 5) were treated with different concentrations of UDP (0 μM, 10 μM, 50 μM and 100 μM) for different times (0 h, 6 h, 12 h and 24 h). The CCK-8 assay showed increased proliferation of RA FLSs in the presence of 10 μM, 50 μM and 100 μM UDP (p = 0.002, 0.0003, and 0.0002, respectively) compared with that in the PBS-treated control group (Fig. 3A). However, the

CCK-8 assay did not show a significant change in the proliferation of OA FLSs in the presence of 10 μM, 50 μM and 100 μM UDP (p = 0.96, 0.90, and 0.81, respectively) compared with that in the PBS-treated control group (Fig. 3B). The Annexin V/PI apoptosis analysis showed that the apoptosis rate of RA FLSs was decreased in the presence of UDP (100 μM) compared with that in the PBS-treated control group (p = 0.0316) (Fig. 3C). However, the Annexin V/PI apoptosis analysis detected little change in OA FLS apoptosis in the presence of UDP (p = 0.3317) compared with that in the PBS-treated control culture (Fig. 3D).

We used wound healing and Transwell assays to evaluate the effect of UDP on the migration of RA FLSs. The wound healing assays showed that RA FLS migration was increased in the presence of UDP (100 μM) (p = 0.0022) compared with that of control FLSs treated with PBS (Fig. 3E). The Transwell assays also showed that RA FLS migration was increased in the presence of UDP (100 μM) (p = 0.004) (Fig. 3F) compared with that of PBS-treated control FLSs. However, the wound healing assay showed only a slight change in OA FLS migration in the presence of UDP (100 μM) (p = 0.59) compared with that of control FLSs treated with PBS (Fig. 3G). The Transwell assay also showed only a slight change in OA FLS migration in the presence of UDP (100 μM) (p = 0.32) compared with that of FLSs treated with PBS (Fig. 3H).

We used flow cytometry to examine proinflammatory cytokine production in the FLS cultures. The assay showed significantly elevated IL-6 levels in the culture medium of RA FLSs in the presence of 100 μM UDP (2203 ± 712.2, p = 0.044), but the concentrations of IL-2, IL-4, IL-10, TNF-α and IFN-γ were not significantly changed (14.04 ± 6.09, p = 0.99; 20.17 ± 14.19, p = 0.59; 29.8 ± 25.13, p = 0.61; 99.47 ± 17.07, p = 0.75; and 18.43 ± 17.61 pg/mL, p = 0., respectively), compared with those in the PBS-treated control culture (861 ± 294.5, 13.95 ± 7.81, 15.97 ± 9.13, 25.53 ± 21.84, 104.2 ± 32.92, and 18.44 ± 11.84 pg/mL, respectively) (Fig. 4A). Compared with those in the control culture (14.3 ± 7.77, 41.9 ± 35.6, 1039 ± 230.2, 19.9 ± 15.6, 86.27 ± 46.17, and 14.87 ± 6.20 pg/mL), the respective concentrations of IL-2, IL-4, IL-6, IL-10, TNF-α and IFN-γ in the culture medium of OA FLSs were not significantly changed in the presence of 100 μM UDP (14.44 ± 12.44, p = 0.98; 43.53 ± 34.55, p = 0.74; 1239 ± 559.4, p = 0.40; 17.73 ± 13.19, p = 0.27; 87.47 ± 37.36, p = 0.85; and 15.33 ± 5.65 pg/mL, p = 0.83) (Fig. 4B).

An IL-6 ELISA was performed to verify the above results. This assay also showed significantly increased IL-6 levels in the culture medium of RA FLSs in the presence of 10 μM, 50 μM and 100 μM UDP (p = 0.022, 0.0205, and 0.0003, respectively) compared with that in samples from cells treated with PBS (Fig. 4C). However, ELISA showed only slight changes in IL-6 levels in the culture medium of OA FLSs in the presence of 10 μM, 50 μM and 100 μM UDP (p = 0.559, 0.088, and 0.010, respectively) (Fig. 4D). The above results indicated that UDP activated RA FLSs and induced IL-6 secretion but did not similarly affect OA FLSs.

Regulation of P2Y6 expression on the effects of UDP

The abundance of P2Y6 mRNA in RA and OA synovial tissue was analyzed in datasets from the GEO database (dataset type: expression profiling by array). The expression data (expression values) of 10

patients with RA and 6 OA controls from dataset GDS5402/208373_s_at, 5 patients with RA and 5 OA controls from dataset GDS2126/38222_at, 10 patients with RA and 10 OA controls from dataset GDS5401/208373_s_at, and 13 patients with RA and 10 OA controls from dataset GDS5403/208373_s_at were analyzed in SPSS software v.21.0. Significantly increased transcription of P2Y6 was found in RA synovial tissues (259.6 ± 24.53, n = 38) compared with OA samples (171.3 ± 18.85, n = 31) (Student's unpaired t-test, p = 0.0076) (Fig. 5A).

In the present study, the expression level of P2Y6 in synovial tissues was also examined by real-time PCR, Western blotting, immunofluorescence and immunohistochemistry. P2Y6 mRNA expression was significantly increased in RA synovial tissues (n = 9) compared with OA synovial tissues (n = 9) (p = 0.0447) (Fig. 5B). In addition, western blot analysis showed that P2Y6 protein expression was significantly increased in RA synovial tissues (n = 5) compared with OA synovial tissues (n = 5) (p = 0.0005) (Fig. 5C). Immunofluorescence analysis of synovial tissues showed that P2Y6 protein expression was significantly increased in RA synovial tissues (n = 5) compared with OA synovial tissues (n = 5) (p = 0.0002) (Fig. 5D). Immunohistochemical analysis showed that P2Y6 protein expression was significantly increased in RA synovial tissues (n = 5) compared with OA synovial tissues (n = 5) (p = 0.0005) (Fig. 5E).

To verify the effect of UDP on RA FLSs, RA FLSs (n = 5) were cultured with both UDP (100 μM) and MRS2578 (10 μM), the chemical inhibitor of P2Y6. Cell proliferation was investigated using RTCA, apoptosis was detected with an annexin V/PI apoptosis assay, and IL-6 secretion was measured using a flow cytometric bead assay. Compared with that of RA FLSs cultured with PBS, RA FLS proliferation was increased in the presence of UDP (p = 0.0007) and was decreased in the presence of MRS2578 alone (p = 0.0017) and of UDP and MRS2578 together (p = 0.0024). The above results demonstrated that RA FLS proliferation was decreased in the presence of MRS2578 alone (p < 0.0001) and of UDP and MRS2578 together (p < 0.0001) (Fig. 6A). Compared with that in the PBS-treated culture, RA FLS apoptosis was decreased in the presence of UDP alone (p = 0.0440), increased in the presence of MRS2578 alone (p = 0.0285), and unchanged in the presence of UDP and MRS2578 together (p = 0.0917). The above results demonstrated that RA FLS apoptosis was increased in the presence of MRS2578 alone (p = 0.0339) and of UDP and MRS2578 together (p = 0.0476) (Fig. 6B). In addition, compared with that in the PBS-treated culture, IL-6 secretion in RA FLSs was increased in the presence of UDP (p = 0.0051) and was decreased in the presence of MRS2578 alone (p = 0.0021) and of UDP and MRS2578 together (p = 0.0023) (Fig. 6C). The wound healing assay showed that compared with that in the PBS-treated control culture, RA FLS migration was increased in the presence of UDP (p = 0.0016) and was decreased in the presence of MRS2578 alone (p = 0.0094) and of UDP and MRS2578 together (p = 0.0007). The above results demonstrated that RA FLS migration was decreased in the presence of MRS2578 alone (p < 0.0001) and of UDP and MRS2578 together (p = 0.0031) (Fig. 6D). Moreover, the Transwell assay showed that compared with that in the PBS-treated control culture, RA FLS migration was increased in the presence of UDP (p = 0.0003) and was decreased in the presence of MRS2578 (p = 0.0088) and of UDP and MRS2578 together (p = 0.0328). The above results demonstrated that RA FLS migration was decreased in the presence of MRS2578 alone (p = 0.0014) and of UDP and MRS2578 together (p = 0.0063) (Fig. 6E).

The effect of UDP on CIA

Rats induced with collagen II were simultaneously injected with UDP, MRS2578 or both UDP and MRS2578. The disease score as assessed by toe swelling was increased, and radiological signs (soft tissue swelling, new bone formation and marginal osseointegration) and histochemical staining were significantly enhanced in CIA rats compared with normal control rats ($p < 0.0001$), indicating successful establishment of CIA in the rats. The disease score was significantly increased in CIA rats treated with UDP ($p = 0.0052$) but decreased in CIA rats treated with MRS2578 ($p = 0.0193$) or both UDP and MRS2578 ($p = 0.0331$) compared with CIA rats. In addition, compared with that in CIA rats treated with UDP, the disease score was decreased in CIA rats treated with MRS2578 ($p = 0.0002$) or with both UDP and MRS2578 ($p = 0.0002$). The disease score did not differ significantly between CIA rats treated with MRS2578 alone and CIA rats treated with both UDP and MRS2578 ($p = 0.7332$) (Fig. 7A, B). Compared with that in normal control rats, paw inflammation in CIA rats was significantly exacerbated, indicating successful establishment of CIA in the rats. Paw inflammation was significantly exacerbated in CIA rats treated with UDP ($p = 0.0058$) but alleviated in CIA rats treated with MRS2578 ($p = 0.024$) or with both UDP and MRS2578 ($p = 0.004$) compared with CIA rats. Compared with that in CIA rats treated with UDP, paw inflammation was alleviated in CIA rats treated with MRS2578 ($p < 0.0001$) or with both UDP and MRS2578 ($p < 0.0001$). Paw inflammation did not differ significantly between CIA rats treated with MRS2578 alone and CIA rats treated with both UDP and MRS2578 ($p = 0.51$) (Fig. 7C).

SF was also collected from rats on day 20 after the first UDP injection, and the cytokine concentrations were measured by flow cytometry. Compared with the corresponding concentrations in the normal control group, the concentrations of IL-6, GM-CSF and TNF-α in the CIA control group were significantly increased ($p = 0.0299$, 0.0250, and 0.0376, respectively), the concentrations of IL-10 were significantly decreased ($p = 0.0317$), and the concentrations of IL-2, IL-4, IL-5, IL-13, and IFN-γ were not significantly changed. Compared with that in CIA rats, the IL-6 level was significantly increased in CIA rats treated with UDP ($p = 0.0053$) but decreased in CIA rats treated with MRS2578 ($p = 0.0040$) or with both UDP and MRS2578 ($p = 0.0114$). Compared with that in CIA rats treated with UDP, the IL-6 level was decreased in CIA rats treated with MRS2578 ($p = 0.0002$) or with both UDP and MRS2578 ($p = 0.0004$). However, the IL-6 level did not differ significantly between CIA rats treated with MRS2578 alone and CIA rats treated with both UDP and MRS2578 ($p = 0.2901$). Moreover, the concentrations of IL-2, IL-4, IL-5, IL-10, IL-13, GM-CSF, IFN-γ and TNF-α did not differ significantly (Fig. 7D). Cytokine expression in the SF of rats was also evaluated by IL-6 ELISA. The IL-6 level was significantly increased in CIA rats treated with UDP ($p = 0.0486$) but decreased in CIA rats treated with MRS2578 ($p = 0.0467$) or with both UDP and MRS2578 ($p = 0.293$) compared with CIA rats. Compared with that in CIA rats treated with UDP, the IL-6 level was decreased in CIA rats treated with MRS2578 ($p = 0.0005$) or with both UDP and MRS2578 ($p = 0.0002$). However, the IL-6 level did not differ significantly between CIA rats treated with MRS2578 alone and CIA rats treated with both UDP and MRS2578 ($p = 0.908$) (Fig. 7E).

We examined UDP levels in the peripheral blood and SF of CIA rats using the fluorescence polarization method. The UDP level in peripheral blood was significantly higher in CIA rats than in normal control rats

(p = 0.0163). Compared with that in CIA rats, the peripheral blood UDP level was significantly increased in CIA rats treated with UDP (p = 0.0482) or both UDP and MRS2578 (p = 0.0362) but was not significantly different in CIA rats treated with MRS2578 (p = 0.3711). Compared with that in CIA rats treated with UDP, the peripheral blood UDP level was decreased in CIA rats treated with MRS2578 (p = 0.0312) but was not significantly different in CIA rats treated with both UDP and MRS2578 (p = 0.9421). The UDP level in peripheral blood was significantly higher in CIA rats treated with both UDP and MRS2578 than in CIA rats treated with MRS2578 (p = 0.0231) (Fig. 8A). The UDP level in SF was significantly higher in CIA rats than in normal control rats (p = 0.0090). Compared with that in CIA rats, the UDP level in SF was significantly increased in CIA rats treated with UDP (p = 0.0066) or both UDP and MRS2578 (p = 0.0074) but was not significantly different in CIA rats treated with MRS2578 (p = 0.4286). Compared with that in CIA rats treated with UDP, the UDP level in SF was decreased in CIA rats treated with MRS2578 (p = 0.0022) but was not significantly different in CIA rats treated with both UDP and MRS2578 (p = 0.5821). Finally, the UDP level in SF was significantly higher in CIA rats treated with both UDP and MRS2578 than in CIA rats treated with MRS2578 alone (p = 0.0019) (Fig. 8B).

We also examined P2Y6 expression in synovial tissues of the model rats by real-time PCR and Western blot analysis. P2Y6 mRNA expression in synovial samples was significantly higher in CIA rats than in normal control rats (p = 0.0017). P2Y6 mRNA expression in synovial tissues did not differ significantly between CIA rats and CIA rats treated with UDP alone (p = 0.196), MRS2578 alone (p = 0.211) or UDP and MRS2578 together (p = 0.721). P2Y6 mRNA expression in synovial tissues did not differ significantly between CIA rats treated with UDP and CIA rats treated with MRS2578 alone (p = 0.0581) or with UDP and MRS2578 together (p = 0.1091). P2Y6 mRNA expression in synovial tissues did not differ significantly between CIA rats treated with MRS2578 alone and CIA rats treated with UDP and MRS2578 together (p = 0.348) (Fig. 8C). However, P2Y6 protein expression in synovial tissues was significantly higher in CIA rats than in normal control rats (p = 0.0049). However, P2Y6 protein expression in synovial tissues did not differ significantly between CIA rats and CIA rats treated with UDP alone (p = 0.476), MRS2578 alone (p = 0.308) or UDP and MRS2578 together (p = 0.545). Moreover, P2Y6 protein expression in synovial tissues did not differ significantly between CIA rats treated with UDP and CIA rats treated with MRS2578 alone (p = 0.128) or with UDP and MRS2578 together (p = 0.267). P2Y6 protein expression in synovial tissues also did not differ significantly between CIA rats treated with MRS2578 alone and CIA rats treated with UDP and MRS2578 together (p = 0.765) (Fig. 8D).

Discussion

In this study, via metabolomic analysis, we found significantly increased UDP levels in RA SF compared with OA SF. We confirmed this finding in blood and SF by comparing samples from 36 RA patients and 36 OA patients using the Transcreener UDP Assay. Furthermore, we found increased levels of UDP in blood and SF from CIA rats compared with normal control rats. These results suggest a high level of UDP in RA and CIA. Furthermore, the UDP level was moderately correlated with the levels of anti-CCP and RF in RA SF, indicating the potential role of UDP in RA.

We continued by investigating the effect of a high UDP level on RA. UDP injection significantly aggravated paw inflammation in CIA rats. Additionally, UDP stimulated the proliferation and migration of RA FLSs *in vitro* and suppressed their apoptosis, indicating the activating effects of UDP on RA FLSs. UDP also increased IL-6 secretion by cultured RA FLSs and in CIA rats but did not affect the production of other cytokines, such as IL-2, IL-4, IL-10, TNF-α and IFN-γ. IL-6 plays a key role in local and systemic manifestations of RA [19]. Blockade of IL-6 has been suggested to be an effective method for RA treatment [20, 21]. The above results suggest that a high UDP level stimulates the pathogenic progression of RA. This study is the first to report the effects of a high UDP level on RA, although many studies have reported that UDP activates inflammatory responses such as phagocytosis and cytokine/chemokine production [17, 22, 23].

UDP plays a role via P2Y6. The human P2Y6 receptor (hP2Y6) is a member of the G protein-coupled pyrimidinergic P2 receptor family that responds specifically to the extracellular nucleotide UDP. P2Y6 is expressed in neutrophils, macrophages, dendritic cells, eosinophils, B cells and T cells and plays roles in apoptosis and cell differentiation, maturation and migration [24]. In our study, we found high P2Y6 expression in RA synovial tissues using real-time PCR, Western blotting and immunohistochemistry. We also found increased expression of P2Y6 in CIA synovial tissues. When RA FLSs were cultured with both UDP and MRS2578, a P2Y6 antagonist, their proliferation and IL-6 secretion were significantly suppressed, and the apoptosis rate was increased. CIA rats injected with MRS2578 or with both UDP and MRS2578 showed decreased paw inflammation and IL-6 production. UDP had little effect on OA FLS proliferation and IL-6 secretion, and P2Y6 expression was relatively low in OA synovial tissues. These observations suggest that UDP plays a stimulatory role in RA via P2Y6. Increased UDP levels and high P2Y6 expression stimulate RA and CIA progression. Targeting P2Y6 receptors might be useful for the treatment of RA. However, UDP did not change P2Y6 expression; P2Y6 protein expression in synovial tissues was not significantly changed in CIA rats treated with UDP alone, MRS2578 alone or UDP and MRS2578 together. The reason that P2Y6 expression is elevated in RA and CIA is unknown. However, high levels of UDP and P2Y6 cooperatively promoted RA pathogenesis.

Extracellular nucleotides (ATP, ADP, UTP and UDP) exert proinflammatory effects through the activation of P2 purinergic receptors such as P2 × 7 and P2Y6 [4,

17, 25]. ATP can act as a danger signal that can cause systemic inflammatory response syndrome [25, 26]. Accumulating evidence has suggested that P2 × 7, a receptor for ATP, is a critical regulator and potential target of RA [27, 28]. UDP is an important extracellular nucleotide signaling molecule implicated in diverse biological processes via specific activation of metabotropic pyrimidine and purine nucleotide receptors (P2Y receptors). Pyrimidine and purine metabolism are components of nucleotide metabolism. Purine metabolism is activated in RA relative to OA [29]. Methotrexate, a first-line drug for RA, can alleviate RA progression by inhibiting pyrimidine metabolism and purine metabolism [30, 31]. Leflunomide, a selective inhibitor of de novo pyrimidine synthesis that alters pyrimidine metabolism, has been successfully used to treat RA and psoriatic arthritis for many years [32, 33]. Lapachol, a compound

targeting pyrimidine metabolism, can ameliorate experimental autoimmune arthritis [34]. These results support our finding indicating the important role of UDP-related nucleotide metabolism in RA.

MRS2578 was found to inhibit the release of IL-6 and IL-8/keratinocyte chemoattractant (IL-8/KC) by lung epithelial cells *in vivo*, whereas intrapulmonary application of the P2Y6 receptor agonist UDP increased the bronchoalveolar levels of IL-6 and KC. In addition, selective activation of P2Y6 receptors was found to induce the secretion of IL-6 and KC/IL-8 by murine and human lung epithelial cells *in vitro* [35]. Application of pressure was found to induce IL-6 expression through the P2Y6 receptor in human dental pulp cells [36]. Treatment with monosodium urate crystals stimulated normal human keratinocytes to produce IL-1α, IL-8/CXCL8, and IL-6 through P2Y6 receptors. In addition, treatment with either P2Y6-specific antagonists or P2Y6 antisense oligonucleotides significantly inhibited the production of IL-1α, IL-8/CXCL8 and IL-6 by human keratinocytes [37]. Activation of the P2Y6 receptor by its natural ligand, UDP, or its specific agonist, MRS2693, led to the production of IL-6 and IL-8 [38]. *In vitro* studies demonstrated that proliferation and IL-6 secretion are P2Y6 receptor-mediated processes in lung fibroblast cells [39]. MRS2578 treatment was found to diminish chronic constriction injury-induced increases in P2Y6 mRNA expression and IL-6 secretion as well as JAK2/STAT3 mRNA expression and phosphorylation modification in spinal cord tissues [40]. UDP was also found to induce the production of the proinflammatory chemokines monocyte chemotactic protein-1 (MCP-1) and Interferon-γ (IFN-γ)-induced protein 10 (IP-10 or CXCL-10) in hP2Y6-transfected promonocytic U937 cells but not in 1321N1 astrocytoma cell lines stably transfected with hP2Y6. Moreover, UDP was found to induce the production of IL-8 but not TNF-alpha in human 1321N1 astrocytoma cells stably transfected with hP2Y6. Therefore, the immunostimulatory effect of UDP/P2Y6/IL-6 signaling on the production of proinflammatory cytokines is selective and cell type-dependent [22]. The above observations support our findings regarding the stimulation of the UDP/P2Y6/IL-6 pathway during RA progression.

In summary, this study showed that the level of UDP is increased in RA and CIA and that UDP stimulates proliferation, cell migration and IL-6 secretion in cultured RA FLSs and CIA rats. Additionally, P2Y6 expression was found to be increased in RA and CIA synovial tissues. Treatment with the P2Y6 antagonist MRS2578 inhibited the effects of UDP on proliferation and IL-6 secretion in RA FLSs and CIA rats. These results suggest that UDP is highly expressed in RA and stimulates RA pathogenesis by promoting P2Y6 activities to increase IL-6 production.

Abbreviations

Anti-CCP
anticyclic citrullinated peptide; CIA:collagen-induced arthritis;
DAB
diaminobenzidine; DEM:differentially expressed metabolites (s).
ELISA
enzyme-linked immunosorbent assay; FC:fold change; FLSs:fibroblast-like synoviocytes; GEO:the Gene Expression Omnibus; HMDB:the Human Metabolome Database; HRP:horseradish peroxidase; IFN-

γ:Interferon-γ; IL-6:interleukin-6; LC-MS:quasi-targeted liquid chromatography-mass spectrometry; MCP-1:monocyte chemotactic protein-1; OA:osteoarthritis; OPLS-DA:orthogonal partial least squares discriminant analysis; P2Y receptors:pyrimidine and purine nucleotide receptors; P2Y6:metabotropic pyrimidine and purine nucleotide receptor pyrimidinergic receptor P2Y, G Protein-Coupled, 6;PVDF:polyvinylidene fluoride membranes; Q-PCR:quantitative real-time PCR; RA:rheumatoid arthritis; RF:rheumatoid factor; ROC:Receiver operating characteristic; RTCA:real-time cell analysis; SDS-PAGE:sodium dodecyl sulfate-polyacrylamide gel electrophoresis; SF:synovial fluid; TOM:topological overlap matrix; UDP:Uridine diphosphate; VIP:variable importance in projection; WB:Western blotting; WGCNA:Weighted gene coexpression network analysis;

Declarations

Acknowledgements

Not applicable.

Authors' contributions

XTC was the principal investigator, designed the study, supervised experiments, and wrote the manuscript. HXW, HW, and KHF performed the experiments. All authors read and approved the final manuscript.

Funding

This study was supported by the Shandong Provincial Key R & D programs

(2017CXGC1202 and GG201703080038).

Availability of data and materials

All relevant data and materials are included in this published article.

Ethics approval and consent to participate

The study protocol was approved by the Medical Ethics Committee of The Affiliated Hospital of Qingdao University (Approval number: 20190302, China). The breeding and care of the experimental animals were carried out in accordance with the Helsinki Convention on Animal Protection and the Regulations of the People's Republic of China on the Administration of Experimental Animals.

Consent for publication

Not applicable.

Competing interests

The authors declare that they have no competing interests.

Author details

1. Medical Research Center of the Affiliated Hospital of Qingdao University. Wutaishan Road 1677, Qingdao, Shandong, 266000. P. R. China.
2. Shandong Provincial Qianfoshan Hospital, Shandong University. Jingshi Road 16766, Jinan, Shandong, 250014. P. R. China.
3. Qingdao Engineering Technology Center For Major Disease Markers Wutaishan Road 1677, Qingdao, Shandong, 266000, P. R. China.

References

1. Smolen JS, Aletaha D, McInnes IB. Rheumatoid arthritis. Lancet. 2016;388(10055):2023–38.
2. Boeynaems JM, Communi D, Gonzalez NS, Robaye B. Overview of the P2 receptors. Semin Thromb Hemost. 2005;31(2):139–49.
3. El-Tayeb A, Qi A, Nicholas RA, Muller CE. Structural modifications of UMP, UDP, and UTP leading to subtype-selective agonists for P2Y2, P2Y4, and P2Y6 receptors. J Med Chem. 2011;54(8):2878–90.
4. Koizumi S, Shigemoto-Mogami Y, Nasu-Tada K, Shinozaki Y, Ohsawa K, Tsuda M, et al. UDP acting at P2Y6 receptors is a mediator of microglial phagocytosis. Nature. 2007;446(7139):1091–5.
5. Parandeh F, Abaraviciene SM, Amisten S, Erlinge D, Salehi A. Uridine diphosphate (UDP) stimulates insulin secretion by activation of P2Y6 receptors. Biochem Biophys Res Commun. 2008;370(3):499–503.
6. Mamedova LK, Joshi BV, Gao ZG, von Kugelgen I, Jacobson KA. Diisothiocyanate derivatives as potent, insurmountable antagonists of P2Y6 nucleotide receptors. Biochem Pharmacol. 2004;67(9):1763–70.
7. Li R, Tan B, Yan Y, Ma X, Zhang N, Zhang Z, et al. Extracellular UDP and P2Y6 function as a danger signal to protect mice from vesicular stomatitis virus infection through an increase in IFN-beta production. J Immunol. 2014;193(9):4515–26.
8. Zhang Z, Wang Z, Ren H, Yue M, Huang K, Gu H, et al. P2Y(6) agonist uridine 5'-diphosphate promotes host defense against bacterial infection via monocyte chemoattractant protein-1-mediated monocytes/macrophages recruitment. J Immunol. 2011;186(9):5376–87.
9. Yu R, Li C, Sun L, Jian L, Ma Z, Zhao J, et al. Hypoxia induces production of citrullinated proteins in human fibroblast-like synoviocytes through regulating HIF1alpha. Scand J Immunol. 2018;87(4):e12654.
10. Nagatani K, Itoh K, Nakajima K, Kuroki H, Katsuragawa Y, Mochizuki M, et al. Rheumatoid arthritis fibroblast-like synoviocytes express BCMA and are stimulated by APRIL. Arthritis Rheum. 2007;56(11):3554–63.

11. Stephenson W, Donlin LT, Butler A, Rozo C, Bracken B, Rashidfarrokhi A, et al. Single-cell RNA-seq of rheumatoid arthritis synovial tissue using low-cost microfluidic instrumentation. Nat Commun. 2018;9(1):791.
12. Wei Z, Wang F, Song J, Lu Q, Zhao P, Xia Y, et al. Norisoboldine inhibits the production of interleukin-6 in fibroblast-like synoviocytes from adjuvant arthritis rats through PKC/MAPK/NF-kappaB-p65/CREB pathways. J Cell Biochem. 2012;113(8):2785–95.
13. Nanki T, Nagasaka K, Hayashida K, Saita Y, Miyasaka N. Chemokines regulate IL-6 and IL-8 production by fibroblast-like synoviocytes from patients with rheumatoid arthritis. J Immunol. 2001;167(9):5381–5.
14. Arnett FC, Edworthy SM, Bloch DA, McShane DJ, Fries JF, Cooper NS, et al. The American Rheumatism Association 1987 revised criteria for the classification of rheumatoid arthritis. Arthritis Rheum. 1988;31(3):315–24.
15. Aletaha D, Neogi T, Silman AJ, Funovits J, Felson DT, Bingham CO 3. 2010 rheumatoid arthritis classification criteria: an American College of Rheumatology/European League Against Rheumatism collaborative initiative. Ann Rheum Dis. 2010;69(9):1580–8. rd, et al.
16. Bayne K. Developing guidelines on the care and use of animals. Ann N Y Acad Sci. 1998;862:105–10.
17. Kim B, Jeong HK, Kim JH, Lee SY, Jou I, Joe EH. Uridine 5'-diphosphate induces chemokine expression in microglia and astrocytes through activation of the P2Y6 receptor. J Immunol. 2011;186(6):3701–9.
18. Liao KP, Batra KL, Chibnik L, Schur PH, Costenbader KH. Anti-cyclic citrullinated peptide revised criteria for the classification of rheumatoid arthritis. Ann Rheum Dis. 2008;67(11):1557–61.
19. Abdel Meguid MH, Hamad YH, Swilam RS, Barakat MS. Relation of interleukin-6 in rheumatoid arthritis patients to systemic bone loss and structural bone damage. Rheumatol Int. 2013;33(3):697–703.
20. Narazaki M, Tanaka T, Kishimoto T. The role and therapeutic targeting of IL-6 in rheumatoid arthritis. Expert Rev Clin Immunol. 2017;13(6):535–51.
21. Md Yusof MY, Emery P. Targeting interleukin-6 in rheumatoid arthritis. Drugs. 2013;73(4):341–56.
22. Cox MA, Gomes B, Palmer K, Du K, Wiekowski M, Wilburn B, et al. The pyrimidinergic P2Y6 receptor mediates a novel release of proinflammatory cytokines and chemokines in monocytic cells stimulated with UDP. Biochem Biophys Res Commun. 2005;330(2):467–73.
23. Grbic DM, Degagne E, Langlois C, Dupuis AA, Gendron FP. Intestinal inflammation increases the expression of the P2Y6 receptor on epithelial cells and the release of CXC chemokine ligand 8 by UDP. J Immunol. 2008;180(4):2659–68.
24. Le Duc D, Schulz A, Lede V, Schulze A, Thor D, Bruser A, et al. P2Y Receptors in Immune Response and Inflammation. Adv Immunol. 2017;136:85–121.
25. Wilhelm K, Ganesan J, Muller T, Durr C, Grimm M, Beilhack A, et al. Graft-versus-host disease is enhanced by extracellular ATP activating P2 × 7R. Nat Med. 2010;16(12):1434–8.

26. Chen CJ, Chang SJ. Purinergic signaling during inflammation. N Engl J Med. 2013;368(13):1260.
27. Stock TC, Bloom BJ, Wei N, Ishaq S, Park W, Wang X, et al. Efficacy and safety of CE-224,535, an antagonist of P2 × 7 receptor, in treatment of patients with rheumatoid arthritis inadequately controlled by methotrexate. J Rheumatol. 2012;39(4):720–7.
28. North RA, Jarvis MF. P2X receptors as drug targets. Mol Pharmacol. 2013;83(4):759–69.
29. Kang KY, Lee SH, Jung SM, Park SH, Jung BH, Ju JH. Downregulation of Tryptophan-related Metabolomic Profile in Rheumatoid Arthritis Synovial Fluid. J Rheumatol. 2015;42(11):2003–11.
30. Smolenska Z, Kaznowska Z, Zarowny D, Simmonds HA, Smolenski RT. Effect of methotrexate on blood purine and pyrimidine levels in patients with rheumatoid arthritis. Rheumatology. 1999;38(10):997–1002.
31. Cutolo M, Sulli A, Pizzorni C, Seriolo B, Straub RH. Anti-inflammatory mechanisms of methotrexate in rheumatoid arthritis. Ann Rheum Dis. 2001;60(8):729–35.
32. Breedveld FC, Dayer JM. Leflunomide: mode of action in the treatment of rheumatoid arthritis. Ann Rheum Dis. 2000;59(11):841–9.
33. Fragoso YD, Brooks JB. Leflunomide and teriflunomide: altering the metabolism of pyrimidines for the treatment of autoimmune diseases. Expert Rev Clin Pharmacol. 2015;8(3):315–20.
34. Peres RS, Santos GB, Cecilio NT, Jabor VA, Niehues M, Torres BG, et al. Lapachol, a compound targeting pyrimidine metabolism, ameliorates experimental autoimmune arthritis. Arthritis Res Ther. 2017;19(1):47.
35. Vieira RP, Muller T, Grimm M, von Gernler V, Vetter B, Durk T, et al. Purinergic receptor type 6 contributes to airway inflammation and remodeling in experimental allergic airway inflammation. Am J Respir Crit Care Med. 2011;184(2):215–23.
36. Satrawaha S, Wongkhantee S, Pavasant P, Sumrejkanchanakij P. Pressure induces interleukin-6 expression via the P2Y6 receptor in human dental pulp cells. Arch Oral Biol. 2011;56(11):1230–7.
37. Uratsuji H, Tada Y, Kawashima T, Kamata M, Hau CS, Asano Y, et al. P2Y6 receptor signaling pathway mediates inflammatory responses induced by monosodium urate crystals. J Immunol. 2012;188(1):436–44.
38. Hao Y, Liang JF, Chow AW, Cheung WT, Ko WH. P2Y6 receptor-mediated proinflammatory signaling in human bronchial epithelia. PLoS One. 2014;9(9):e106235.
39. Muller T, Fay S, Vieira RP, Karmouty-Quintana H, Cicko S, Ayata CK, et al. P2Y6 Receptor Activation Promotes Inflammation and Tissue Remodeling in Pulmonary Fibrosis. Front Immunol. 2017;8:1028.
40. Bian J, Zhang Y, Liu Y, Li Q, Tang HB, Liu Q. P2Y6 Receptor-Mediated Spinal Microglial Activation in Neuropathic Pain. Pain Res Manag. 2019;2019:2612534.

Figures

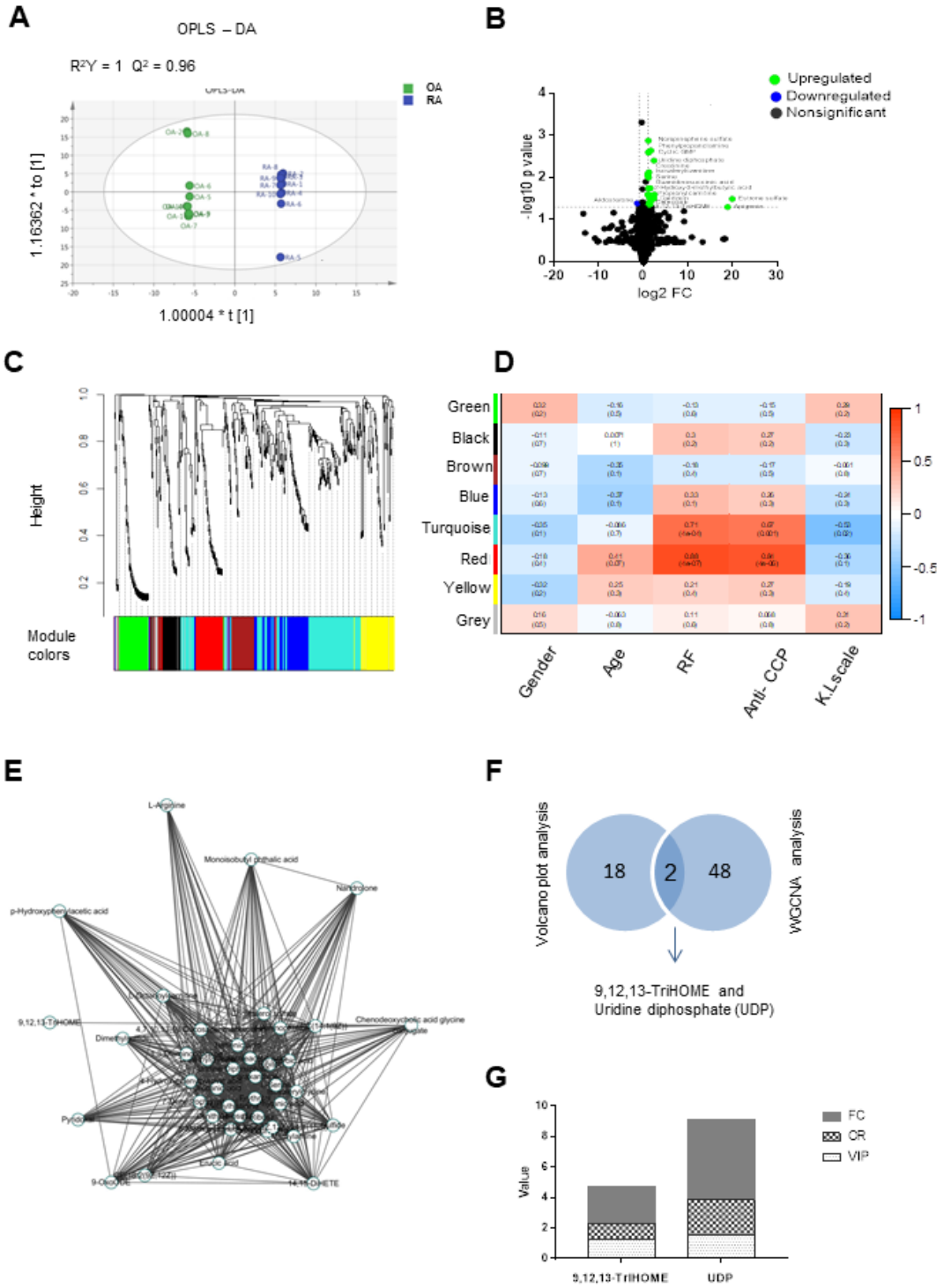

Figure 1

Multivariate statistical analysis of SF samples. (A) OPLS-DA of SF. (B) Volcano plots indicating the statistical significance of metabolite changes between OA and RA ($p < 0.05$; FC >2). (C) Clustering dendrograms of the metabolite set. (D) Correlation of metabolite coexpression network modules with clinical features of RA. (E) Metabolite expression network derived from the red module. (F) Venn diagrams of key metabolites in the volcano plot analysis and WGCNA sets. SF: synovial fluid.

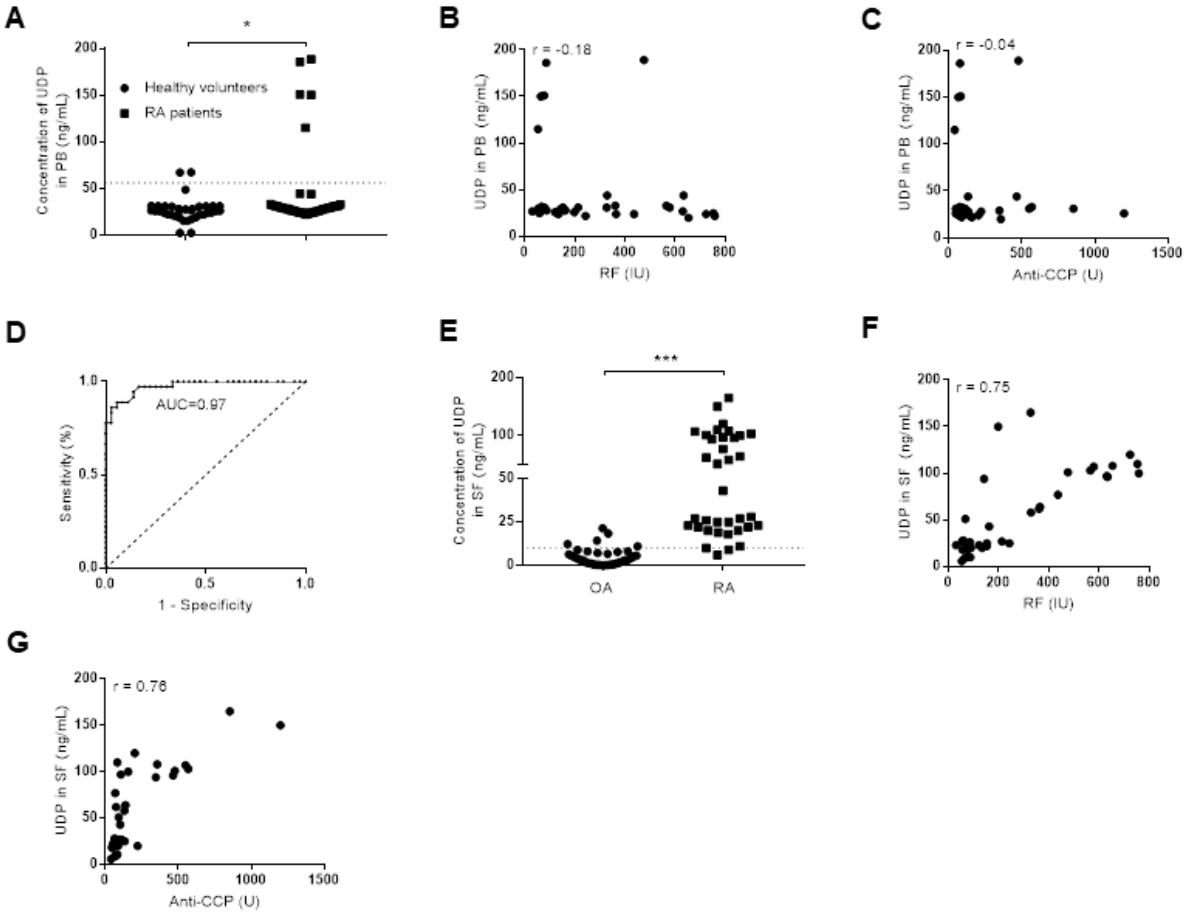

Figure 2

UDP levels in RA. (A) The UDP level in RA plasma was measured using a Transcreener UDP assay. (B) Association analysis of the UDP level with the serum RF level. (C) Association analysis of the PB UDP level with the serum anti-CCP level. (D) ROC analysis of UDP in RA SF. € The UDP level in RA SF was measured using a Transcreener UDP assay. (F) Association analysis of the SF UDP level with the serum RF level. (G) Association analysis of the SF UDP level with the serum anti-CCP level. SF: synovial fluid. PB: peripheral blood.

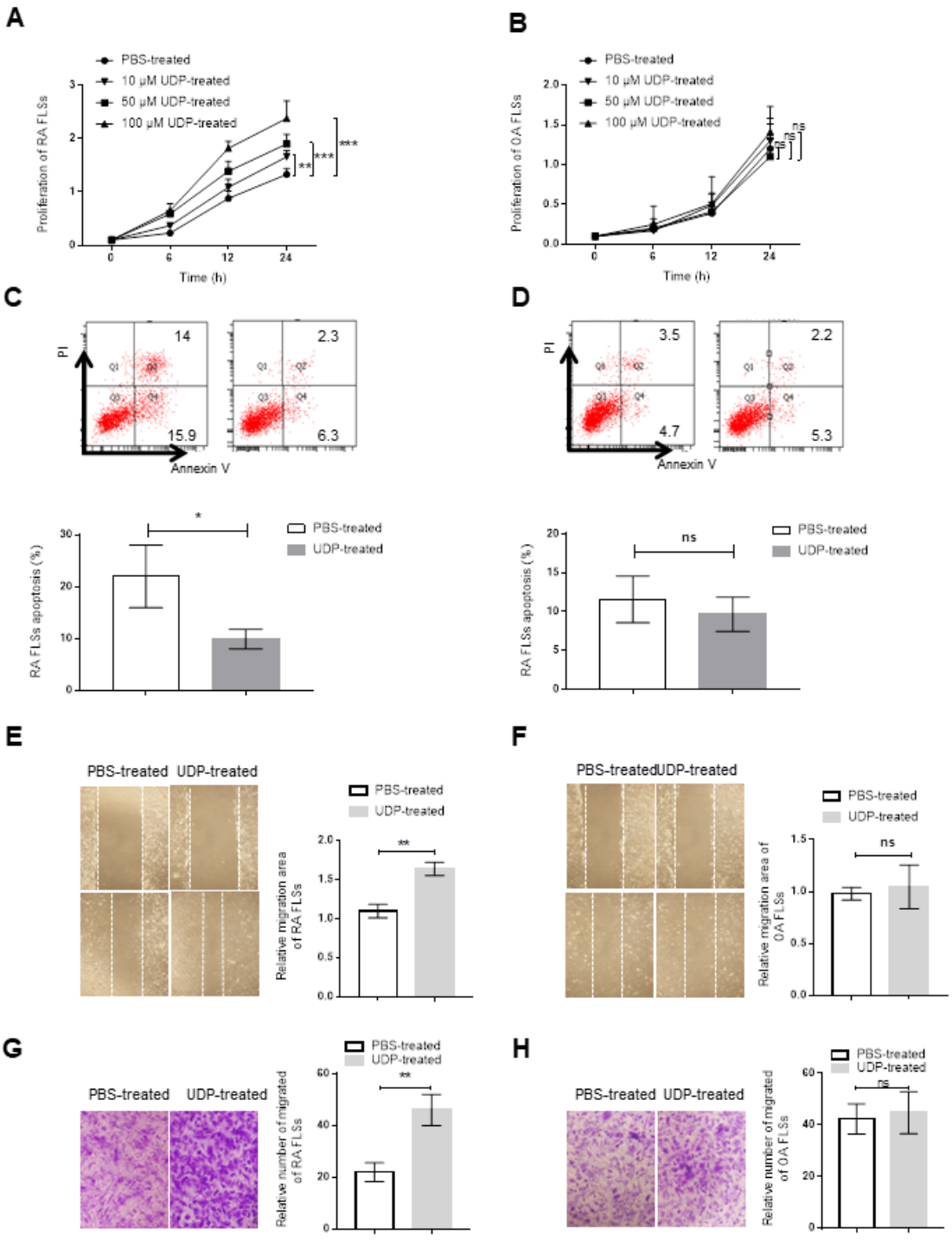

Figure 3

Effect of UDP on RA FLSs. (A) RA FLS proliferation was assessed using a CCK-8 assay and statistical analysis. (B) OA FLS proliferation was assessed using a CCK-8 assay and statistical analysis. (C) RA FLS apoptosis was assessed using flow cytometry and statistical analysis. (D) RA FLS apoptosis was assessed using flow cytometry and statistical analysis. (E) RA FLS migration was assessed using a wound healing assay. (F) RA FLS migration was assessed using a Transwell assay. (G) OA FLS migration

was assessed using a wound healing assay and statistical analysis. (H) OA FLS migration was assessed using a Transwell assay and statistical analysis. *p<0.05, **p<0.01, and ***p<0.001.

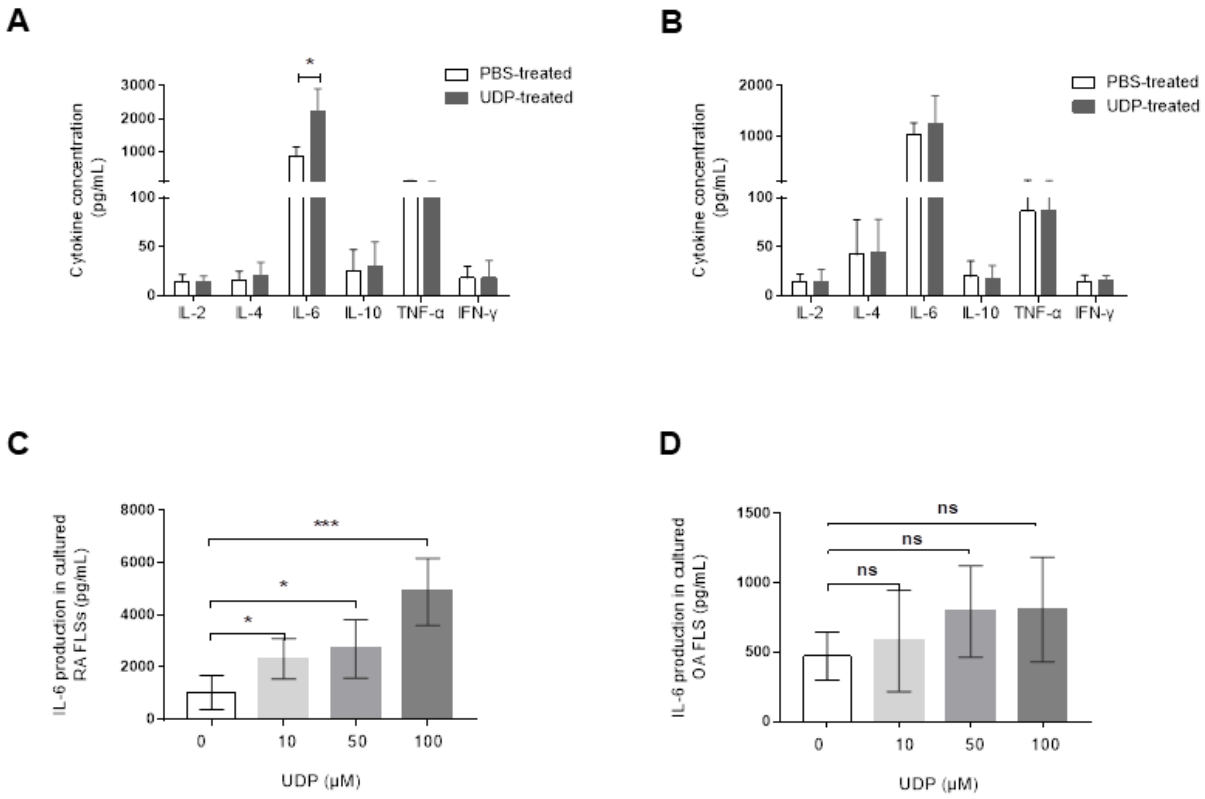

Figure 4

Effect of UDP on RA FLS cytokine secretion. (A) Cytokine secretion by RA FLSs was assessed using a flow cytometric bead assay. (B) Cytokine secretion by OA FLSs was assessed using a flow cytometric bead assay. (C) IL-6 secretion by RA FLSs was assessed using ELISA and statistical analysis. (D) IL-6 secretion by OA FLSs was assessed using ELISA and statistical analysis. *p<0.05, **p<0.01, and ***p<0.001.

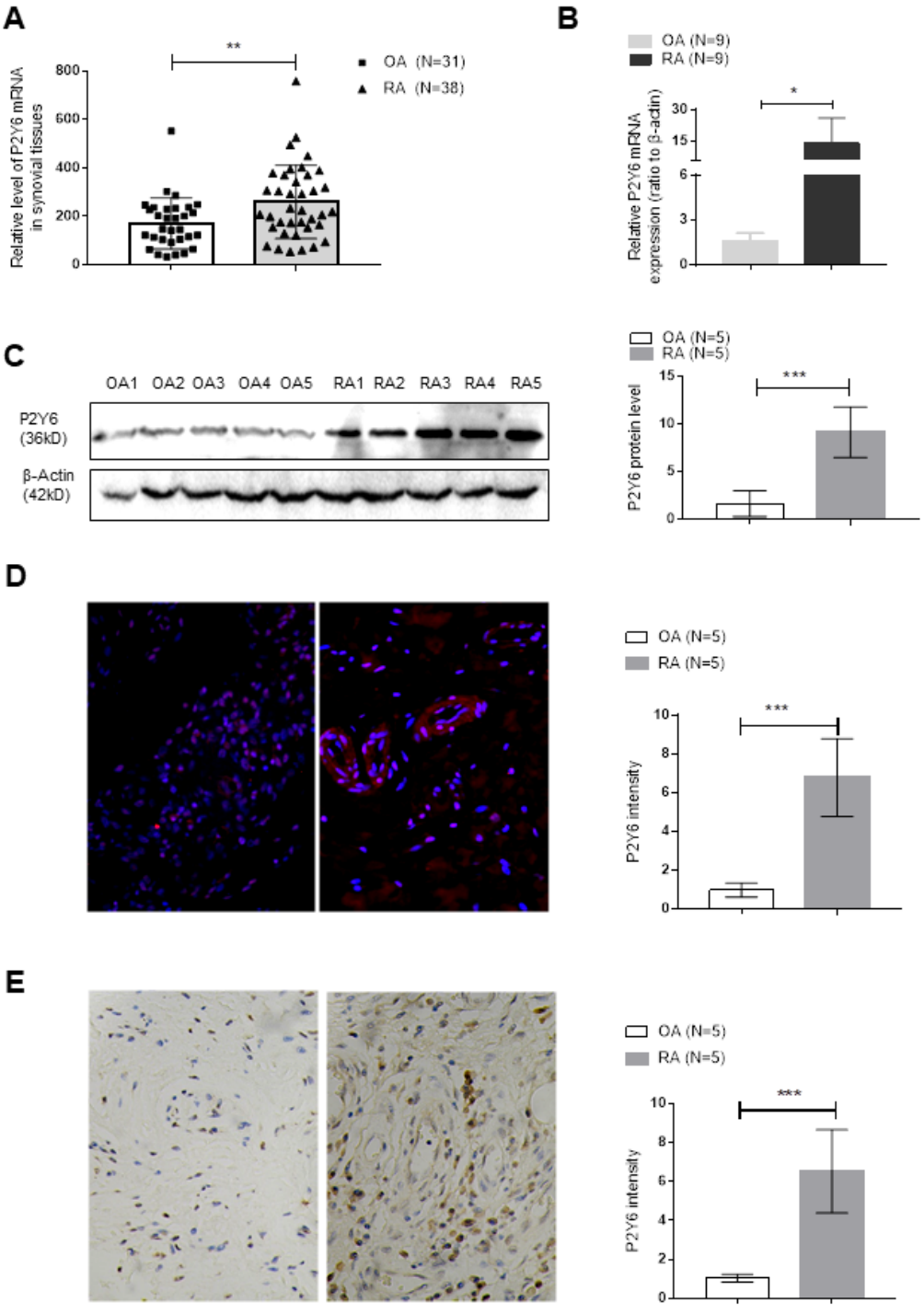

Figure 5

P2Y6 expression in RA synovial tissues and cultured FLSs. (A) P2Y6 expression was analyzed in the GEO database, which included RA synovial tissue (n=38) and OA (n=31) synovial tissue microarray data. P2Y6 was overexpressed in RA synovial tissue compared with OA synovial tissue. (B) P2Y6 expression in SF from RA or OA samples was assessed using Q-PCR. (C) P2Y6 expression in FLSs from RA and OA samples was assessed using western blotting and statistical analysis. (D) P2Y6 expression in human RA

and OA synovial tissues was assessed using immunofluorescence and statistical analysis. (E) P2Y6 expression in RA and OA human synovial tissues was assessed using immunohistochemical staining and statistical analysis.

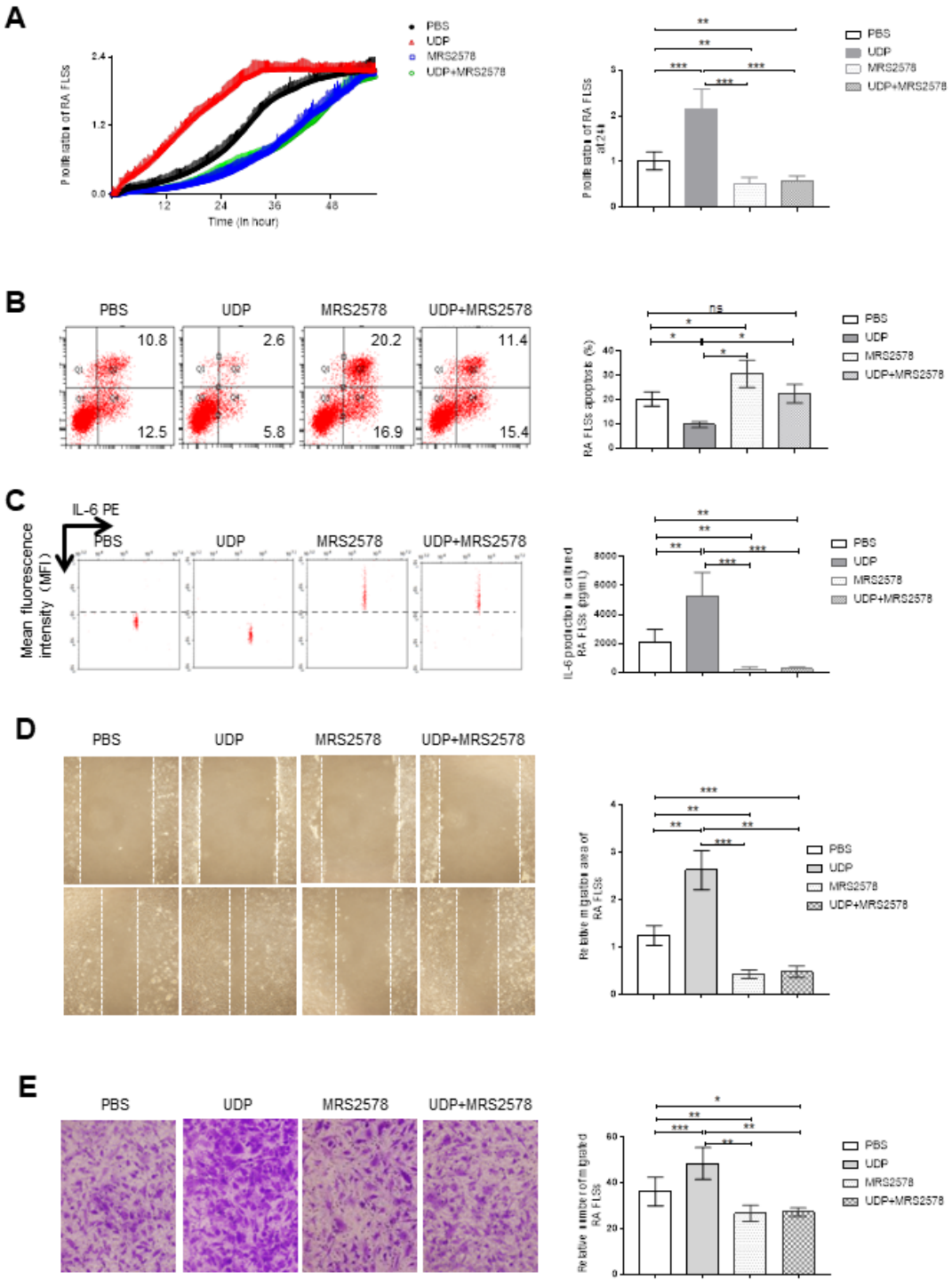

Figure 6

Effect of MRS2578 on proliferation and IL-6 levels in cultured RA FLSs. Cultured RA FLSs were treated with UDP (100 μM) and/or MRS2578 (10 μM). (A) Cell proliferation was assessed using RTCA and

statistical analysis. (B) Apoptosis was assessed using flow cytometry and statistical analysis. (C) IL-6 secretion was assessed using a flow cytometric bead assay and statistical analysis. (D) The migration of RA FLSs was assessed using a wound healing assay and statistical analysis. (E) RA FLS migration was assessed using a Transwell assay and statistical analysis. *p < 0.05, **p < 0.01; ***p < 0.001.

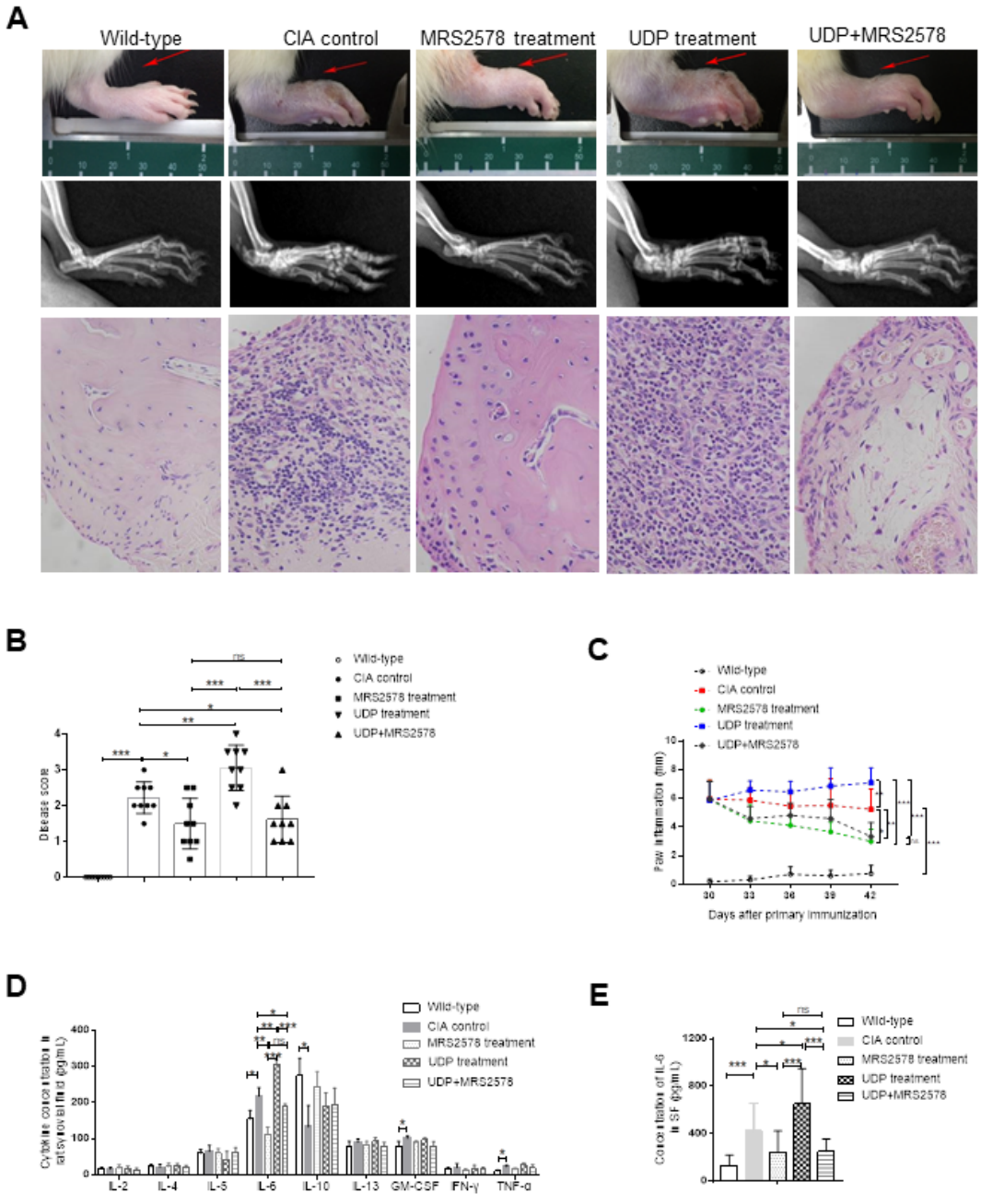

Figure 7

Effect of the P2Y6 inhibitor on CIA rats treated with UDP. (A) X-ray images and histochemical staining images of joint inflammation in CIA rats treated with UDP and/or MRS2578. (B) Disease scores were quantified based on histologic evidence. (C) Inflammation curve analysis based on paw inflammation. (D) Cytokine release into rat PB was assessed using a flow cytometric bead assay. (E) Cytokine release in rat SF using a flow cytometric bead assay. (F) IL-6 release into rat SF was assessed using ELISA. *p<0.05, **p<0.01, and ***p<0.001.

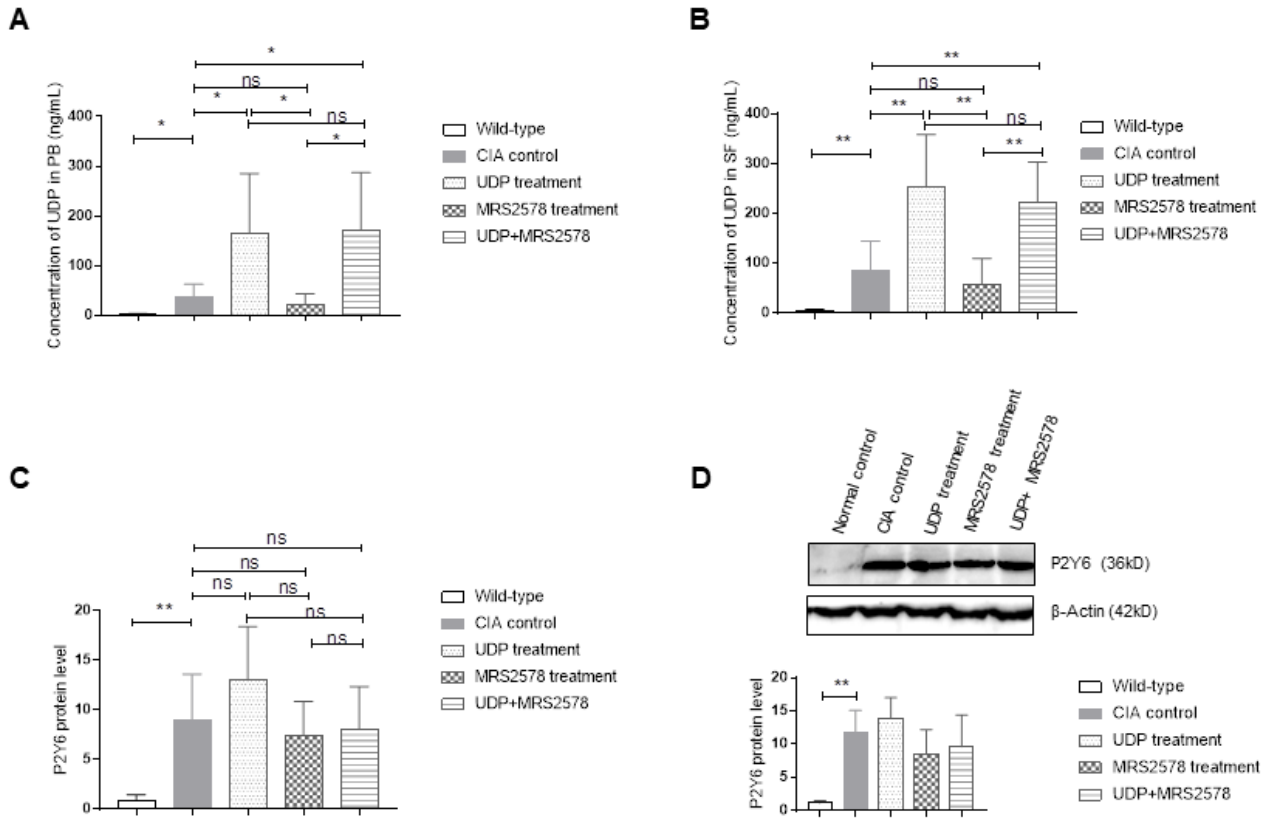

Figure 8

UDP level in SF and P2Y6 expression in synovial tissues of CIA rats. (A) The UDP level in CIA rat PB was assessed using fluorescence polarization analysis. (B) The UDP level in CIA rat SF was assessed using fluorescence polarization analysis. (C) P2Y6 expression in synovial tissue was assessed using real-time PCR. (D) P2Y6 expression in CIA synovial tissues was assessed using western blotting and statistical analysis.

Supplementary Files

This is a list of supplementary files associated with this preprint. Click to download.

- SupplementaryTable2S49V7.doc
- SupplementaryTable1S49V7.doc